

PAPER • OPEN ACCESS

Dynamic reconfiguration of active distribution network considering multiple active management strategies

To cite this article: Wei Bao *et al* 2019 *IOP Conf. Ser.: Earth Environ. Sci.* **227** 032036

View the [article online](#) for updates and enhancements.

Dynamic reconfiguration of active distribution network considering multiple active management strategies

Wei Bao¹, Shaohui Zhang¹, Yichen Song^{2,3}, Mingqiang Wang², Xiao Li², Yuehao Yan¹ and Xiaoyong Fu¹

¹ State Grid Zhengzhou Power Supply Company, Zhengzhou, China;

² Key Laboratory of Power System Intelligent Dispatch and Control of Ministry of Education (Shandong University), Jinan, China.

³ Email: yichensongsdu@foxmail.com

Abstract. To make full use of various active management resources in ADN to improve the economic efficiency, a dynamic reconfiguration model of active distribution network considering multiple active management (AM) strategies is proposed in this paper. The AM strategies including the configuration of energy storage system, output power controlling of distributed generation, reactive power compensation with static var compensators and packet capacitor switching, tap adjusting with on-load tap changer, and demand side response management. The model tries to minimize the total costs with respect to various operating constraints. Several linearization techniques are applied to formulate the dynamic reconfiguration problem into a mixed-integer linear programming (MILP) model, which guarantees global optimal solution and also reduces the computational difficulty significantly. Finally, the validity and effectiveness of the proposed dynamic reconfiguration model is verified on the IEEE 33-node distribution network system.

1. Introduction

Active distribution network (ADN) has become a new development trend of smart distribution network, which could cope with the increasing high penetration of distributed generation in distribution network by using various kinds of advantaged technologies [1]. ADN is an effective way to realize active control and active management of various distributed energy sources [2] such as distributed generation (DG), energy storage system (ESS), demand side management (DRM), static var compensators (SVC), packet capacitor switching (SC), tap adjusting with on-load tap changer (OLTC), etc.

Distribution network has quantities of sectionalizing switches and tie switches, and distribution network reconfiguration (DNR) can be achieved by changing the open/closed status of these switches to optimize network operation level[3]. DNR is an important component of distribution management system and an effective way to reduce power loss, balancing load demand and improve voltage quality[4-5]. DNR can be divided into two categories: static reconfiguration and dynamic reconfiguration. The static reconfiguration is applied under a determined power flow or a certain operation mode[3,6]. However, the actual load in distribution network is time varying. So it is necessary to introduce the dynamic reconfiguration which applies the continuous adjustment of the network topology over a given period of time to fit for the actual operation of distribution network. Dynamic reconfiguration means that the distribution system operators (DSO) can dynamically change



the topology of the distribution network by altering the state of the remote control switch, thereby achieving flexible network structure optimization[7]. In [8], a new method for dynamic reconfiguration to maximize loadability of radial distribution systems is presented, and it is solved by a fuzzy adaptation of the evolutionary programming algorithm. In [9], a day-ahead and real-time optimal dispatch model considering energy storage and controllable distributed generation of ADN is built, and an improved particle swarm optimization algorithm is adopted to solve the models. In [10], a day ahead scheduling model considering the flexible load, the energy storage, reactive power compensation devices is built. And multi-objective particle swarm optimization algorithm is used to solve this problem.

However, the existing papers about dynamic reconfiguration rarely consider AM strategies or just consider part of them, which don't make the most of their economic value to optimize the economy operation of ADN. Meanwhile, the papers mentioned above use different kind of intelligent algorithm to solve MINLP problem, which could only get locally optimal solution and the convergence speed is slow and they depend on specific system parameters.

The contributions of this paper are as follows.

1) A dynamic reconfiguration of ADN considering multiple AM strategies is proposed. The model consider comprehensive AM strategies (the configuration of ESS, output power controlling of DG, reactive power compensation with SVC and packet SC, tap adjusting with OLTC, and DRM), which could reduce the operation cost more efficiently.

2) Various linearization methods are applied to transform the MINLP model are difficult to solve into a MILP model, which could be solved with high computing efficiency. And different from the intelligent algorithm, MILP can get globally optimal solution with less iterations and is adapt to wildly varying circumstances.

2. Dynamic reconfiguration of ADN

In this section, the formulation of the dynamic reconfiguration of ADN is presented. The model considered multiple active management strategies with various operation constraints. The optimization model is set up as follows:

2.1. Objective function

The objective function of this model is to minimize total operation cost:

$$\min f = C^{GRID} + C^{DG} + C^{ESS} + C^{DRM} \quad (1)$$

The meaning and calculation method of each part of the objective function in equation (1) are as follows:

1) Power purchase cost

$$C^{GRID} = \sum_{t \in N_T} C^P \cdot P_t^{GRID} \quad (2)$$

where N_T is the set of look-ahead time periods (e.g., 24 h); C^P is the electricity price; and P_t^{GRID} is the active power purchased from substation during time t .

2) DG operation cost

$$C^{DG} = \sum_{i \in N_{DG}} \sum_{t \in N_T} C^{DG} \cdot P_{i,t}^{DG} \quad (3)$$

where N_{DG} is the set of DG; C^{DG} is the operation and maintenance cost of DG; and $P_{i,t}^{DG}$ is the output power of the i th DG during time t .

3) DRM cost

$$C^{DRM} = \sum_{i \in N_{DRM}} \sum_{t \in N_T} C^{DRM} \cdot P_{i,t}^{DRM} \quad (4)$$

DRM measures in this paper refer to common interruptible load (IL) measures. ILs are attracted to sign a contract with DSO to interrupt or reduce their demand during peak load or emergency with certain economic compensation. In (4), N_{DRM} is the set of DRM; C^{DRM} is the compensation cost of IL; and $P_{i,t}^{DRM}$ is the interruptible load of the i th object of DRM during time t .

4) ESS cost

$$C^{ESS} = \sum_{i \in N_{ESS}} \sum_{t \in N_T} C^{ESS} \cdot (P_{i,t}^C + P_{i,t}^D) \quad (5)$$

where N_{ESS} is the set of ESS; C^{ESS} is the cost of ESS; $P_{i,t}^C$ and $P_{i,t}^D$ are the charging power and discharging power of the i th ESS during time period t , respectively.

2.2. Constraints

1) Power balance constraint

$$P_{i,t}^{GRID} + \sum_{i \in N_{DG}} P_{i,t}^{DG} + \sum_{i \in N_{ESS}} P_{i,t}^D + \sum_{(k,i) \in N_B} z_{ki,t} P_{ki,t} = \sum_{(i,j) \in N_B} z_{ij,t} P_{ji,t} + \sum_{i \in N_L} P_{i,t}^L - \sum_{i \in N_{DRM}} P_{i,t}^{DRM} + \sum_{i \in N_{ESS}} P_{i,t}^C, \forall i, t \quad (6)$$

$$Q_{i,t}^{GRID} + \sum_{i \in N_{DG}} Q_{i,t}^{DG} + \sum_{i \in N_{SVC}} Q_{i,t}^{SVC} + \sum_{i \in N_{SC}} Q_{i,t}^{SC} + \sum_{(k,i) \in N_B} z_{ki,t} Q_{ki,t} = \sum_{(i,j) \in N_B} z_{ij,t} Q_{ji,t} + \sum_{i \in N_L} Q_{i,t}^L, \forall i, t \quad (7)$$

$$P_{ij,t} = U_{i,t} U_{j,t} (G_{ij} \cos \theta_{ij,t} + B_{ij} \sin \theta_{ij,t}) - U_{i,t}^2 G_{ij}, \forall i, t \quad (8)$$

$$Q_{ij,t} = U_{i,t} U_{j,t} (G_{ij} \sin \theta_{ij,t} - B_{ij} \cos \theta_{ij,t}) + U_{i,t}^2 B_{ij}, \forall i, t \quad (9)$$

In the equations, N_B is the set of all branches; N_L is the set of buses connected to loads; N_{SVC} is the sets of buses connected to SVC; N_{SC} is the sets of buses connected to SC; $P_{ki,t}$ and $Q_{ki,t}$ are the active and reactive power flowing from the upstream branches to bus i during time t , respectively; $P_{ij,t}$ and $Q_{ij,t}$ are the active and reactive power flowing to the downstream branches from bus i during time t , respectively; $P_{i,t}^L$ and $Q_{i,t}^L$ are the load active and reactive power of bus i during time t , respectively; $Q_{i,t}^{GRID}$ is the reactive power injected from the substation located at bus i during time t ; $Q_{i,t}^{DG}$ is the reactive power injected from the DG located at bus i during time t ; $Q_{i,t}^{SVC}$ and $Q_{i,t}^{SC}$ are the reactive power compensated by SVC and SC during time t , respectively; $U_{i,t}$ and $U_{j,t}$ are the voltage magnitude of bus i and bus j during time t respectively; $\theta_{ij,t}$ is the phase angle difference between bus i and bus j ; G_{ij} and B_{ij} are the conductance and susceptance of branch ij during time t , respectively.

2) Radial topology constraint

$$\sum_{(i,j) \in N_B} z_{ij,t} = N_i - 1, \forall i, t \quad (10)$$

The status of the switch is defined by the binary variable $z_{ij,t}$, which takes 1 if the switch is closed in period t and takes 0 otherwise. And N_i is the set of all buses.

3) Branch capacity constraint

$$(P_{ij,t})^2 + (Q_{ij,t})^2 \leq (S_{ij})^2, \forall ij, t \quad (11)$$

where S_{ij} is the apparent power capacity of branch ij .

4) Voltage magnitude constraint

$$U_i^{\min} \leq U_{i,t} \leq U_i^{\max}, \forall i, t \quad (12)$$

where U_i^{\min} and U_i^{\max} are the lower and upper limit of voltage magnitude at bus i .

5) Reactive compensation constraint

$$Q_i^{SVC, \min} \leq Q_{i,t}^{SVC} \leq Q_i^{SVC, \max}, \forall i, t \quad (13)$$

$$Q_{i,t}^{SC} = y_{i,t}^{SVC} \cdot Q_{i,t,step}^{SC}, \forall i, t \quad (14)$$

$$y_{i,t}^{SVC} \leq Y_i^{SVC, \max}, \forall i, t$$

Equation (13) is the reactive power output of SVC limits, where $Q_i^{SVC, \min}$ and $Q_i^{SVC, \max}$ are the lower and upper limit of reactive power output of the i th SVC. Equation (14) is the output constraints of SC, where $y_{i,t}^{SVC}$ is the number of groups of SC putted into operation; $Q_{i,t,step}^{SC}$ is the compensating power of

each capacitor group; and $Y_i^{SVC,max}$ is the upper limit of group numbers of SC connected to bus i during period t .

6) OLTC constraint

$$T_i^{OLTC,min} \leq T_{i,t}^{OLTC} \leq T_i^{OLTC,max}, t \in T, \forall i, t \quad (15)$$

where $T_{k,t}$ is the location of transformer tap during period t .

7) Output power controlling of DG

$$\begin{aligned} P_{i,t}^{DG,min} &\leq P_{i,t}^{DG} \leq P_{i,t}^{DG,max}, \forall i, t \\ Q_{i,t}^{DG} &= P_{i,t}^{DG} \cdot \tan \theta_i^{DG}, \forall i, t \\ \theta_i^{DG,min} &\leq \theta_i^{DG} \leq \theta_i^{DG,max}, \forall i, t \end{aligned} \quad (16)$$

where $P_{i,t}^{DG,min}$ and $P_{i,t}^{DG,max}$ are the lower and upper limits of active power output of the i th DG during period t . The constraints setting DG operate in the maximum operating point tracking mode to make full use of renewable resources, and the reactive power output of DG can be adjusted continuously within the allowable range of power factor constraints.

8) ESS constraint

$$0 \leq P_{i,t}^C \leq \rho_{i,t}^C P_i^{ESS,max} \quad (17)$$

$$0 \leq P_{i,t}^D \leq \rho_{i,t}^D P_i^{ESS,max} \quad (18)$$

$$\rho_{i,t}^C + \rho_{i,t}^D \leq 1 \quad (19)$$

$$SOC_{i,t}^{ESS} = SOC_{i,t-1}^{ESS} + \mu^C \rho_{i,t}^C - \mu^D \rho_{i,t}^D \quad (20)$$

$$SOC_i^{ESS,min} \leq SOC_{i,t}^{ESS} \leq SOC_i^{ESS,max} \quad (21)$$

where $P_i^{ESS,max}$ is the maximum charging/discharging power of the i th ESS; $\rho_{i,t}^C$ and $\rho_{i,t}^D$ are binary variables representing the charging/discharging state of ESS, respectively; μ^C and μ^D are the charging/discharging efficiency of ESS, in this paper, their values are 0.9; $SOC_i^{ESS,min}$ and $SOC_i^{ESS,max}$ are the lower and upper limits of state of charge (SOC).

9) DRM constraint

$$0 \leq P_{i,t}^{DRM} \leq P_i^{DRM,max} \quad (22)$$

where $P_i^{DRM,max}$ is the upper limit for IL.

3. Linearization techniques used in the method

Take the linearization method in [11], constraints (8) and (9) can be approximated by the following linear expressions:

$$P_{ij,t} = (U_{i,t} + U_{j,t} - \frac{\theta_{ij,t}^2}{2} - 1)G_{ij} - (2U_{i,t} - 1)G_{ij} + B_{ij}\theta_{ij,t} \quad (23)$$

$$Q_{ij,t} = -(U_{i,t} + U_{j,t} - \frac{\theta_{ij,t}^2}{2} - 1)B_{ij} + (2U_{i,t} - 1)B_{ij} + G_{ij}\theta_{ij,t} \quad (24)$$

Furthermore, the quadratic term $\theta_{ij,t}^2$ in the above equations can be piecewise linearized by 2L blocks and the linearization of absolute sign proposed in [12]:

$$|\theta_{ij,t}| = \sum_{l=1}^L \theta_{ij,t}^-(l) \quad (25)$$

$$\theta_{ij,t}^2 = \sum_{l=1}^L k_{ij}(l)\theta_{ij,t}^-(l) \quad (26)$$

$$|\theta_{ij,t}| = \theta_{ij,t}^+ + \theta_{ij,t}^- \quad (27)$$

$$\theta_{ij,t} = \theta_{ij,t}^+ - \theta_{ij,t}^- \quad (28)$$

$$\theta_{ij,t}^+ \geq 0, \theta_{ij,t}^- \geq 0 \quad (29)$$

where $k_{ij}(l)$ and $\theta_{ij,t}(l)$ are the slope and value of the l th block of $\theta_{ij,t}$, respectively.

Constraint (11) is a circular constraint, which can be approximated by an inscribed regular polygon[11] as shown in Figure 1.

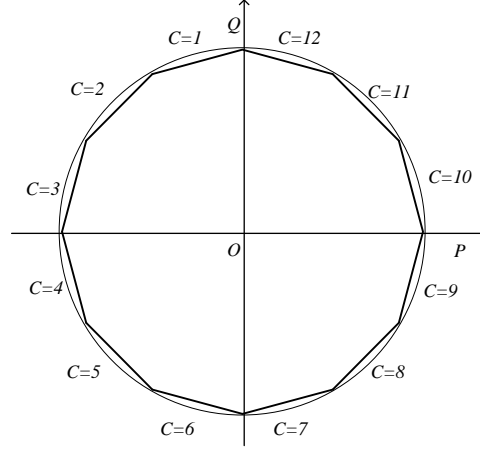


Figure 1. Circular constraint linearization method.

Constraint (11) can be reformulated as:

$$\gamma_{k0}P_{ij,t} + \gamma_{k1}Q_{ij,t} + \gamma_{k2}S_{ij,t}^{\max} \leq 0, k = 1, 2, \dots, 12 \quad (30)$$

where $\gamma_{k0}, \gamma_{k1}, \gamma_{k2}$ are the coefficient corresponding to the linearization circular constraint.

The nonlinear terms $z_{ki,t}P_{ki,t}$, $z_{ij,t}P_{ji,t}$, $z_{ki,t}Q_{ki,t}$ and $z_{ij,t}Q_{ji,t}$ in constraints (6) and (7) can be approximated by the following linear expressions:

$$z_1 = z_{ij,t} * P_{ki,t} \quad (31)$$

$$z_{ij,t} * P_{ki,t}^{\min} \leq z_1 \leq z_{ij,t} * P_{ki,t}^{\max} \quad (32)$$

$$P_{ki,t} - (1 - z_{ij,t})P_{ki,t}^{\max} \leq z_1 \leq P_{ki,t} - (1 - z_{ij,t})P_{ki,t}^{\min} \quad (33)$$

The rest three terms can be reformulated similarly.

4. Case study

The proposed model is tested on modified IEEE 33-bus radial distribution system [4] which consists of 5 tie switches and 32 sectionalize switches. The network diagram proposed is shown in Figure 2. Furthermore, a WT is installed in node 24, a SVC device is installed in node 3, a SC device is installed in node 30, and an ESS device is installed in node 21. And the load curve is presented in Figure 3. All tests are solved by using CPLEX of GAMS on a personal computer with an Intel Core: i5-6400 2.70 GHz CPU and 8 GB of RAM.

The optimization horizon in the evaluation studies is 24 h. The minimum and maximum voltage limits are set to 0.95 pu and 1.05 pu, respectively. The electricity price adopted peak-valley-flat electricity price, the price is 0.83 ¥/kWh at peak period (10:00-16:00, 18:00-22:00), 0.49 ¥/kWh at flat period (08:00-10:00, 16:00-18:00, 22:00-24:00) and 0.17 ¥/kWh at valley period (00:00-08:00). The operation cost of DG, cost of ESS and the cost of DRM are set to 0.2 ¥/kWh, 1.0 ¥/kWh and 0.8 ¥/kWh, respectively, and stay constant during all periods.

The remote-controlled switches are s11, s13, s14, s16, s27, s28, s33, s34, s35, s36, s37, s38.

The optimal configuration of the feeder can be obtained using the proposed approach, as summarized in Table 1, where the opened switches are listed for each time interval and the remainder of the switches is closed. The minimum total cost is ¥53837, of which the DRM cost is ¥1224 and the ESS cost is ¥1337. The calculation time is 02'33".

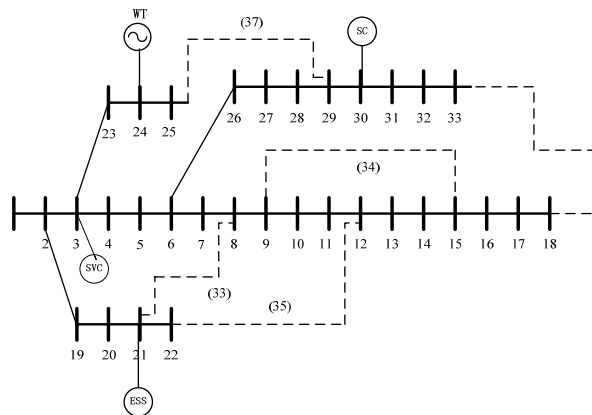


Figure 2. Modified IEEE 33-bus distribution system.

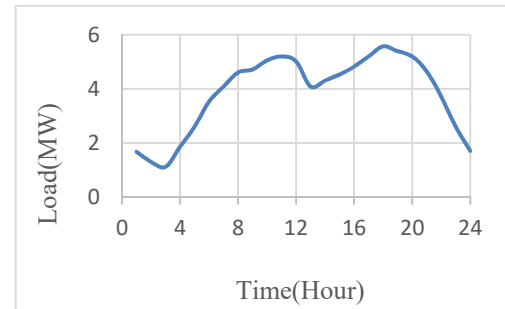


Figure 3. Total load curve.

Table 1. Optimal configuration results of dynamic reconfiguration.

Time	Open switches	Time	Open switches
0-1	s11, s13, s16, s27, s33	12-13	s11,s16, s27, s33, s35
1-2	s11, s13, s16, s27, s33	13-14	s11,s16, s27, s33, s35
2-3	s10, s13, s16, s27,s33	14-15	s11,s16, s27, s33, s35
3-4	s10, s13, s16, s27,s33	15-16	s13,s16, s27, s33, s35
4-5	s13, s16, s27, s33, s35	16-17	s13,s16, s27, s33, s35
5-6	s13, s16, s27, s33, s35	17-18	s13, s16, s28, s33, s35
6-7	s13, s16, s27, s33, s35	18-19	s11, s16, s27, s33, s35
7-8	s13, s16, s27, s33, s35	19-20	s11, s16, s27, s33, s35
8-9	s13, s16, s27, s33, s35	20-21	s11,s16, s27, s33, s35
9-10	s13, s16, s27, s33, s35	21-22	s13,s16, s27, s33, s35
10-11	s11, s16, s27, s33, s35	22-23	s11,s13, s16, s27, s33
11-12	s11, s16, s27, s33, s35	23-24	s11, s13, s16, s27, s33

Without considering AM strategies, the total cost of dynamic DNR is ¥54003. Compared with ¥53837 of dynamic DNR with AM strategies, the total cost decreases 0.3%, i.e., AM strategies can save ¥166 for one day, corresponding to ¥60590 for a year, which is a significant cost saving.

5. Conclusions

This paper proposed a dynamic reconfiguration model with the objective function of minimizing total operation costs. The model applies multiple AM strategies to optimal the economy of system operation, which could better reflect the development requirements of ADN and accord with the trend of future smart distribution network. The 33-bus case verified that AM strategies can significantly increase economic benefits to ADN by comparing with dynamic DNR without AM strategies. During the model solving process, multiple linearization methods are adopted to convert the MINLP model into a MILP problem, which can be easily solved by commercial solver and can guarantee both effectiveness and validity of the solution.

Acknowledgement

This paper is supported by National Natural Science Foundation of China (51407106).

References

- [1] Fan Mingtian, Zhang Zuping, Su Aoxue, et al 2013 Enabling technologies for active distribution systems *Proceedings of the CSEE* **33(22)** 12-18(in Chinese)
- [2] You Yi, Liu Dong, Yu Wenpeng, et al 2012 Technology and its trends of active distribution network *Automation of Electric Power Systems* **36(18)** 10-16
- [3] Baran M E, Wu F F 1989 Network reconfiguration in distribution systems for loss reduction and load balancing *IEEE transactions On Power Delivery* **4(4)** 1401-1407
- [4] Li Zhen-kun, Chen Xingying, Yu Kun, et al 2008 Hybrid particle swarm optimization for distribution network reconfiguration *Proceedings of the CSEE* **28(31)** 35-41
- [5] Civanlar S, Grainger J, Yin H, Lee S S July 1988 Distribution feeder reconfiguration for loss reduction *IEEE Trans on Power Delivery* **3** 1217-1223
- [6] Wu Y, Lee C, Liu L and Tsai S July 2010 Study of Reconfiguration for the Distribution System With Distributed Generators in *IEEE Transactions on Power Delivery* **25(3)** 1678-1685
- [7] Capitanescu F, Ochoa L F, Margossian H, et al 2015 Assessing the potential of network reconfiguration to improve distributed generation hosting capacity in active distribution systems *IEEE Transactions on Power Systems* **30(1)** 346-356
- [8] Venkatesh B, Ranjan R, Gooi H B 2004 Optimal reconfiguration of radial distribution systems to maximize loadability *IEEE Transactions on Power Systems* **19(1)** 260-266
- [9] X Hua, T Lulu, Z Ning, Z Jian and S Qian 2018 Coordinated optimal dispatch for active distribution network under multi-time scales 2018 *13th IEEE Conference on Industrial Electronics and Applications (ICIEA)*, Wuhan. 695-699. doi: 10.1109/ICIEA.2018.8397803
- [10] Yang X, Xia Mingchao, Chen Youyuan, et al 2017 Multi-objective Day Ahead Optimization Scheduling of Regional Active Distribution Network *Proceedings of the 19th Annual Meeting of the China Association for Science and Technology* 1-9 (in Chinese)
- [11] Sun Hao, Zhang Lei, Xu Hailin, et al 2015 Mixed Integer Programming Model for Microgrid Intra-day Scheduling *Automation of Electric Power Systems* **14(1)** 302-317 DOI: 10.7500/AEPS20141117011
- [12] Li X, Wang M, Xu H Active distribution network planning considering linearized system loss[C] *IOP Conference Series: Earth and Environmental Science*. 121. 052072. 10.1088/1755-1315/121/5/052072.2018:052072